

# Electrochemical conditioning of fractal topographies at the silicon oxide/silicon interface

M. Lublow and H. J. Lewerenz

Division of Solar Energy  
Interface Engineering Group  
Hahn-Meitner-Institut Berlin GmbH  
D-14109 Berlin, Germany

## Abstract

On n-type silicon photoelectrodes, immersed in concentrated ammonium fluoride, fractal etch patterns are observable at anodic potentials near 6V. The formation of these patterns was investigated in dependence upon light intensity. For low photon flux, and correspondingly low density of electron-hole pairs, the etch structures exhibit random dendritic branching. For medium photon flux, regular patterns are achieved preserving, e.g., the four-fold symmetry of Si(100) surfaces. At increased light intensities, a transition to chaotic corrosion was found. Model considerations relate the rate of oxide formation to the strength and homogeneity of local stress and strain forces exerted onto silicon bonds. Numerical simulations of strain- and stress-induced crack propagation, carried out in dependence upon light intensity and oxidation rate respectively, are reproducing the structures in good agreement with experimental data.

Self-organized microstructuring at the silicon oxide/silicon interface is a phenomenon inherent to the electrochemical treatment of silicon electrodes in fluoride containing solutions. Well known, e.g., is the formation of nano- and micropores in the n-Si/HF system obtained by anodic polarization and back-side illumination [1]. Also, pores of periodically changing aspect ratio are created during anodic current oscillations in diluted NH<sub>4</sub>F [2], as clearly observed by Transmission Electron Microscopy (TEM) and Atomic Force Microscopy (AFM) [3].

The majority of theoretical models, developed thus far in order to analyze these findings, focus on a complex interaction of local and global parameters in both space and time. Accordingly, pores are considered as specific charge transfer pathways, and efforts were almost successful in understanding the formation of the stunning pore geometries that show a clear dependence upon the silicon crystal orientation.

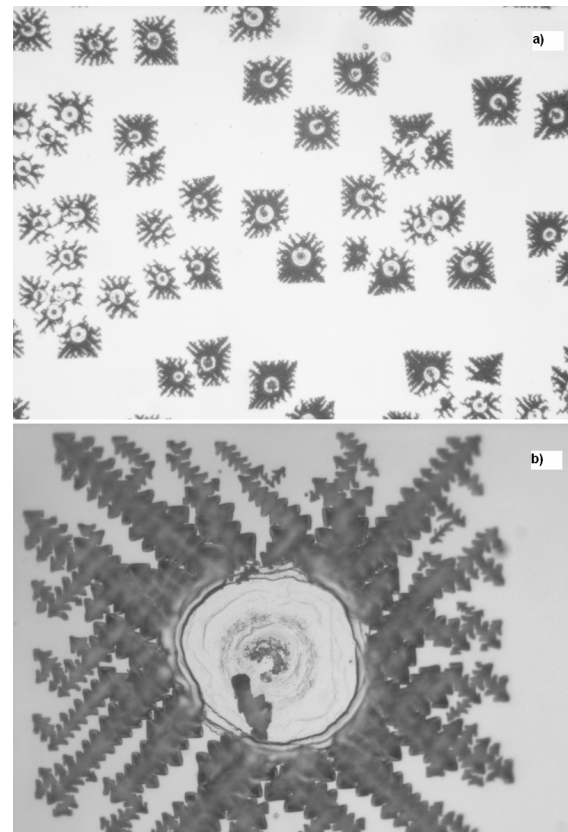


**Fig. 1:** Etch domains on n-Si(100) after 10 min in 40% NH<sub>4</sub>F at 6V; light intensity 7.5mW/cm<sup>2</sup>: a) ~2mm x 2.5mm micrograph; b) ~200µm x 250µm micrograph.

In contrast to this vertical pore formation, novel lateral effects on silicon were recently observed in concentrated NH<sub>4</sub>F solutions where the (anisotropic) etching rate is enhanced by higher supply of OH<sup>-</sup>/F<sup>-</sup> ions [4]. Depending on the fine-tuning of external parameters such as illumination intensity (generation of electron-hole pairs in n-Si), a large variety of fractal etching geometries was produced. Under certain conditions, the surface lattice structure of the respective (111), (100), (110), or (113)

surfaces, is reproduced on a micrometer-scale. For example, etch domains on Si(100) exhibit the four-fold symmetry of the surface lattice almost perfectly (Fig. 1). First model considerations suggest an important influence of oxide-induced stress and strain for both initial crack formation and subsequent propagation along crystal axes (Fig. 2). Variations of thickness and homogeneity of the oxide result in local gradients of stress and strain forces provoking either the straight prolongation of a crack or the change of its direction.

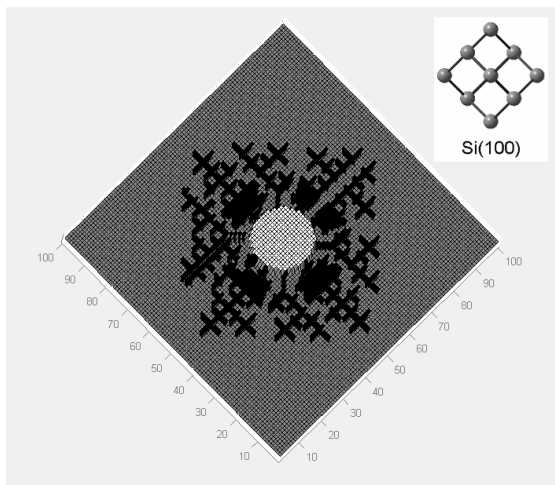


**Fig. 2:** Simulated crack propagation on Si(100) on a 100x100 square grid with center oxide island. Both dendritic branching and boundary orientation (with respect to the surface lattice) are reproduced.

In the case of almost homogeneous oxide coverage, the branching of cracks is thought to proceed from initially built defective sites with almost uniform velocity in all directions. Those defective sites were experimentally observed at the boundaries of oxide islands, built during the initial phase and covered instantly with oxygen bubbles. The assumed uniform speed of crack propagation would result then in a 45°-rotation of the outer boundary of a crack domain when a (100) lattice geometry is considered (see Figs. 1 and 2). For the numerical simulation, the bond-breaking probability due to the strain field was taken into account in a recursion algorithm, restricting the computations to a nearest-neighbor approach [5].

Stochastic crack formation, obtained at lower light intensities, suggest, in turn, a presence of local variations of both oxide thickness and corresponding stress and strain forces (Fig. 3).

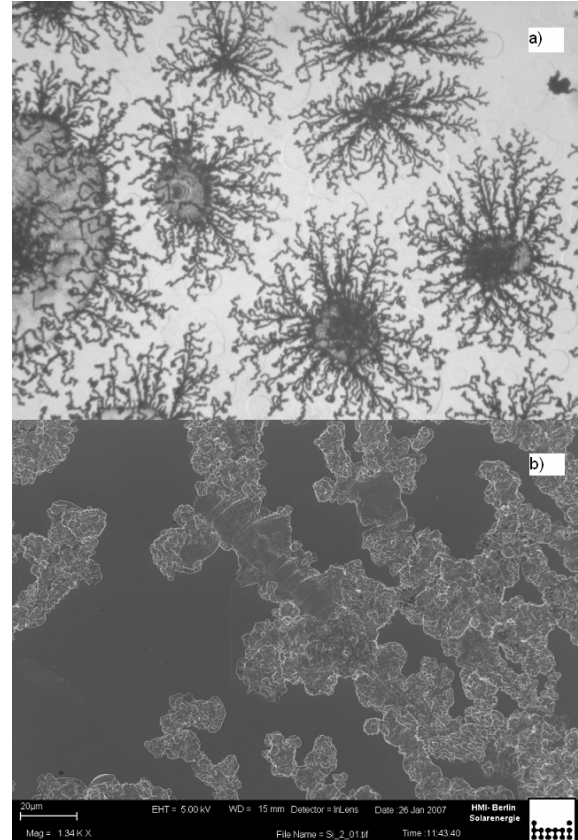


**Fig. 3:** Branching etch grooves on n-Si(111) after 10min exposure to 40% NH<sub>4</sub>F at constant potential of 6V, light intensity 5mW/cm<sup>2</sup>: a) ~2mm x 2.5mm micrograph; b) magnified HR-SEM image of dendrites.

The inhomogeneity of the surface oxide for such samples was already proven earlier by comparison of photoelectron spectroscopy results and dark current measurements near the open circuit potential of Si in 40% NH<sub>4</sub>F. This current is induced by electron injection into the semiconductor conduction band on oxide free surface areas. It was found that the oxide on some areas was etched considerably faster than on others, a result which is not observable on homogeneous oxide layers [4]. The computer simulation of crack propagation in the presence of such irregular stress and strain fields results in ramifying structures similar to those obtained by application of

Diffusion Limited Aggregation (DLA) theory [6].

While a few assumptions seem to be sufficient to model the two-dimensional crack propagation, the conditions for the three-dimensional formation of stable microfacets within the cracks appear rather intricate (Fig. 4).

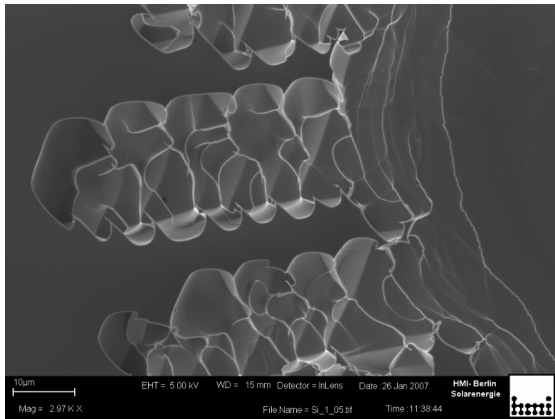
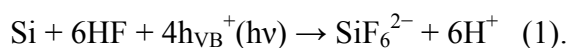


**Fig. 4:** Partial view of a hexagonal structure on n-Si(111). Magnification of a secondary-electron HR-SEM image.

It is basic understanding to describe the overall reaction for the n-Si dissolution in  $\text{NH}_4\text{F}$  under illumination and at higher anodic potentials according to the tetravalent reaction scheme:



Eq. (1) involves an electrochemical oxidation step with subsequent chemical dissolution of the oxide. The depicted ensemble of microfacets in a Si(111) crack (Fig. 4) suggests, however, preferential etching along specific crystallographic directions which goes beyond the mechanism described by Eq. (1). Moreover, observations on Si(100) indicate a continued modification of the inner topography of these cracks while spreading further across the surface. In the case of Si(100), a saw-tooth cross-sectional profile was measured along a crack line first. At later times, an ensemble of microfacets with smaller inclination towards the main (100) plane was found. It appears that passivated facets, i.e., stable areas resisting

to accelerated dissolution, are formed under control of a feedback to the local strain field. Future model considerations have therefore to combine the effects of silicon bond-breaking probabilities in the presence of strain and stress and the existence of stable facets, resulting in the formation of recurring patterns within cracked areas. Atomistic Monte Carlo Simulations already turned out to yield a suitable tool to simulate these anisotropic features, as in the case of wet chemical silicon etching [7], and will be applied in refined computer assisted calculations.

It should be finally noted that the lateral crack formation, described here, has a remarkable correspondence to the initiation and growth of vertical macropores [8]. Beside lattice dependent propagation of single pores, the aggregation of pore ensembles in regular domains on semiconductors other than silicon has been described recently [9]. The effect of surface oxides as a reason for strain-induced forces which may determine (to a certain degree) the observed etch geometries was not considered yet and will be studied in further detail in an upcoming work.

## References

- [1] J. Carstensen, M. Christophersen, G. Hasse, H. Föll, *Phys. Stat. Sol. A* **183** (2000) 63.
- [2] J. Grzanna, H. Jungblut, H. J. Lewerenz, *J. Electroanal. Chem.*, **486** (2000) 190.
- [3] M. Aggour, M. Giersig, H. J. Lewerenz, *J. Electroanal. Chem.*, **383** (1995) 67.
- [4] M. Lublow and H. J. Lewerenz, *Electrochem. and Solid-State Lett.*, **10** (2007) C51-C55.
- [5] P. Meakin, G. Li, L.M. Sander, E. Louis, F. Guinea, *J. Phys. A: Math. Gen.*, **22** (1989) 1393.
- [6] T. Witten and L. Sandler, *Phys.Rev. Lett.*, **47** (1981) 1400.

- [7] M. A. Gosálvez and R. M. Nieminen,  
*New J. Phys.*, **5** (2003) 100.1.
- [8] M. Christophersen, J. Carstensen, S.  
Rönnebeck, C. Jäger, W. Jäger, H. Föll,  
*J. Elec. Soc.*, **148** (2001) E267.
- [9] S. Langa, J. Carstensen, M. Christophersen,  
K. Steen, S. Frey, I. M. Tiginyanu, H. Föll  
*J. Elec. Soc.*, **152** (2005) C525.